Experimental Mechanics (2008) 48:799–807
DOI 10.1007/s11340-008-9137-1

A Pulse-Heated Kolsky Bar Technique for Measuring the Flow Stress of Metals at High Loading and Heating Rates

S.P. Mates · R. Rhorer · E. Whitenton · T. Burns · D. Basak

Received: 10 October 2007 / Accepted: 3 March 2008 / Published online: 5 April 2008

Abstract The National Institute of Standards and Technology (NIST) has developed an electrical pulse-heated Kolsky Bar technique for measuring the constitutive response of metals at heating rates of up to 6,000 K/s and strain rates up to 10^4 s^{-1}. Under these conditions, which are approaching those found in high speed machining, thermally activated microstructural processes such as grain growth, solid state phase transformation and dislocation annealing can be bypassed, leading to unique non-equilibrium superheated microstructural states. Flow stresses can thus differ significantly from equilibrium high temperature conditions. This paper describes the NIST pulse-heated Kolsky bar technique in detail, including a thorough assessment of uncertainties in temperature and flow stress measurement.

Keywords Kolsky-Bar · Split-Hopkinson bar · High heating rate · Flow stress measurement · High strain rate

S.P. Mates (✉)
Metallurgy Division, MSEL,
National Institute of Standards and Technology,
Gaithersburg, MD, USA
e-mail: smates@nist.gov

R. Rhorer (SEM member) ·
E. Whitenton (SEM member)
Manufacturing Metrology Division, MEL,
National Institute of Standards and Technology,
Gaithersburg, MD, USA

T. Burns
Mathematical and Computational Sciences Division, ITL,
National Institute of Standards and Technology,
Gaithersburg, MD, USA

D. Basak
Orbital Sciences Corp.,
Dulles, VA, USA

Introduction

The need to understand the constitutive behavior of metals subjected to rapid thermal and mechanical loading arises from a desire to model extreme physical processes such as high-speed machining [1], explosive impact or other highly dynamic thermo-mechanical events. Simulations of these events can yield valuable insights that may lead to improved cutting processes, or better blast resistant structures with dramatically reduced development cost. However, to be of value, these simulations require accurate constitutive descriptions of the materials involved for the relevant mechanical and thermal loading rates.

While there are well established methods for mechanical testing under rapidly applied loading, less attention has been paid to the response of metals subjected to rapid heating and loading combined. The flow stress of a metal that is subjected to a rapid temperature change can differ significantly from its equilibrium response due to time-dependent thermally-activated microstructural changes. Very fast heating can bypass normal thermal evolution in the microstructure, such as grain growth and solid state phase transformations, leading to unique, non-equilibrium superheated microstructural states. Similarly, dislocation networks that would otherwise respond to elevated temperatures do not have sufficient time to do so when heating times are short. These thermally-activated, time-dependent phenomena can cause rapidly-heated metals to exhibit different flow stresses under rapid loading than the same metal heated slowly and then subjected to rapid loading.

Elevated temperature Kolsky Bar testing is usually performed by heating the sample with a miniature furnace or an induction heating coil [2]. Heating times associated with these techniques are typically measured in minutes. The NIST pulse-heating system can reach temperatures

over 1,000 K in less than a second. These rapid heating rates are achieved by pulsing electrical current directly through the sample as it sits fixed between the compression bars. The sample temperature is controlled using a fast-response infrared pyrometer as a feedback sensor connected to a specialized modulated battery power supply. A prior publication has described the heating method in detail and its performance capabilities [3]. The present paper covers additional aspects of this measurement technique, including a description of the procedures required to compute the stress–strain response of the specimen taking into account the graphite foil layers that are needed to facilitate the rapid sample heating. In addition, a complete uncertainty analysis of temperature and stress–strain measurement results is provided. Finally, the role of the foil in facilitating direct yield strength measurements using the Kolsky bar technique is discussed.

NIST Pulse-Heated Kolsky Bar

The NIST pulse-heated Kolsky bar, shown in Fig. 1, consists of a compression testing arrangement outfitted with an electrical heating circuit to rapidly heat the sample. The compression bars measure 1.5 m long by 1.5 cm diameter and are made of maraging steel. Compression pulses are produced using a gas gun/striker bar arrangement. Electrical current is conducted directly through the sample using the ends of the bars themselves as the electrodes. The heating circuit is connected to the compression bars using low-friction graphite bushings approximately 8 cm from either side of the sample. A bank of 2.5-V lead-acid batteries connected in series provides the electrical power. The maximum power that can be delivered to the sample is controlled by varying the number of batteries in the circuit. The number of batteries therefore determines the maximum heating rate attainable. In a typical test, the sample will draw 400 A of current at 2 V, for a power dissipation of 0.8 kW.

An important advantage of this fast heating technique is that the bars do not heat up significantly during a test (less than 25°C for tests up to 1,000°C within 3 s) because the heating times are very short and the bars are much larger than the sample. A 25°C temperature rise changes the elastic modulus of steel by less than 1% [4], which is not enough to alter the results within the experimental precision of this technique, as described later. If longer heating times are desired and the bar temperature increase is more significant, corrections of the type discussed in [5] can be applied.

The sample temperature is controlled using a millisecond resolution Near Infrared Micro PYrometer (NIMPY) that serves as a feedback sensor for the power supply. The NIMPY consists of an NA 0.14 objective lens and an InGaAs detector. Coupled with a current pre-amplifier, the operational range of the NIMPY is 300°C to 1,000°C. Modulation of the power output is accomplished using a large parallel assembly of field-effect transistors (FETs) and a 2,400 A current switch. For set-point temperature control, the current is rapidly switched to maintain a constant NIMPY voltage signal. Several temperature control methods are

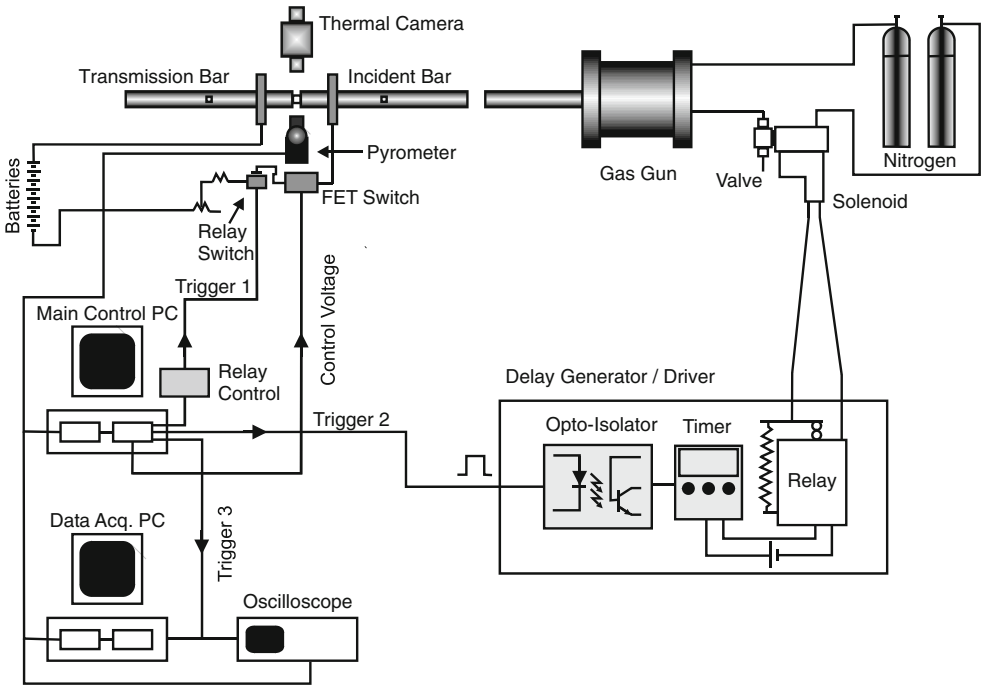

Fig. 1 Temperature control schematic for the NIST pulse-heated compression Kolsky bar technique

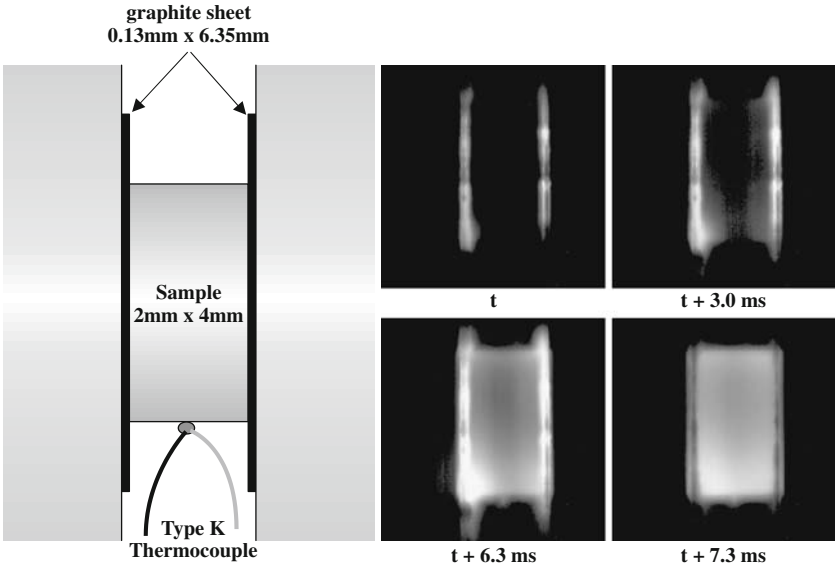

Fig. 2 Sample heating arrangement showing graphite foil inserts and thermocouple placement (*left*) and typical heating behavior revealed by high speed visible light video recording (*right*)

available, including a transient timed test, a transient maximum temperature test, or a proportional-derivative (PD) constant temperature test.

In the PD control mode, the radiance temperature of the sample can be held to within ±3°C (2σ) for any desired length of time. Further details regarding the heating method and typical performance data are given elsewhere [3].

The primary challenge to implementing this direct electrical pulse-heating method is achieving uniform, repeatable heating of the sample and avoiding damaging electrical arcing. Temperature uniformity is essential for a valid compression test. Achieving it is possible only if the contact conductance between the sample and the bars is also uniform. In practice this is difficult to achieve between bare, hard metal surfaces that are only lightly pressed together. With bare contacting surfaces, electrical conduction takes place over the few small areas where the surfaces are in intimate contact, and arcing is unavoidable. To improve the contact uniformity and reduce the chances for arcing, a thin graphite foil is inserted between the sample and the bars as shown in Fig. 2. The foil material, called Grafoil, is manufactured by Graftech.[1] It is both compliant and conductive. The foil fills the void space between the sample and the bars while maintaining good electrical conductivity. This material was chosen among several others, including conductive paint, soft copper foil, electro-deposited gold and sprayed graphite, due to its ability to deliver reliable and uniform heating while suppressing electrical arcing.

The foil pads measure 6.25 mm in diameter by 0.13 mm thick. Alcohol wipes are used to remove dirt and grease from the contacting surfaces prior to installing the sample. The sample plus foil assembly is then placed under slight compression by elastic bands fixed on each bar. When properly assembled, the resistance of the entire assembly ranges between 0.5 Ω and 2 Ω (including a short length of each bar). Because resistance of the interfaces is high compared to the inherent resistance of the sample or the ends of the bars, electrical heating is initially concentrated in the foil. Figure 2(b) reveals how the foil heats first, after which the thermal wave moves into the sample from either side. After this initial transient heating period, the sample temperature becomes uniform. High speed infrared camera measurements indicate that the radiance temperature varies by as little as 20°C (2σ) over the sample profile, as shown in Fig. 3(a). Some of this variation is likely due to roughness or oxidation that changes the surface emissivity, suggested by the mottled appearance of the bottom of the sample. Figure 3(b) shows an occasion where a large thermal gradient developed due to a misaligned sample that resulted in non-uniform contact conductance. Methods for detecting misaligned samples without the aid of infrared camera data, necessary to ensure quality measurements, are discussed later.

Figure 4 shows a typical experiment to illustrate the high degree of control over sample temperature that can be achieved with this technique. In this experiment the sample is first heated to an intermediate radiance temperature of 285°C to establish good thermal conduction, then heated to the final test radiance temperature of 525°C and held constant for a short time (2.4 s) prior to the arrival of

[1] Commercial products are identified in this work to adequately specify certain procedures. In no case does such identification imply recommendation or endorsement by NIST, nor does it imply that the materials or equipment identified are necessarily the best available for the purpose.

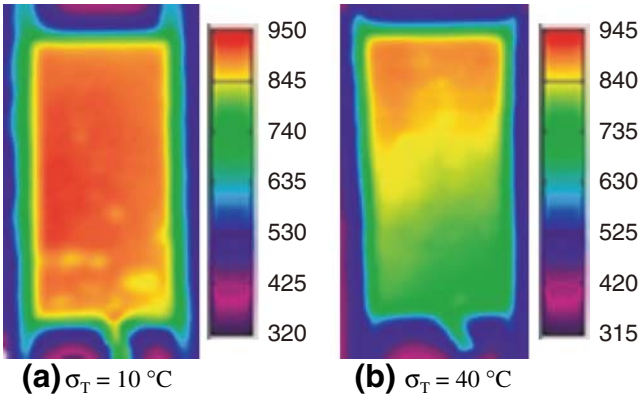

Fig. 3 Sample temperature uniformity revealed by high speed infrared thermal camera showing (**a**) uniform conductance and (**b**) non-uniform conductance. Temperature scales are in degrees Celsius

compression pulse. Pre-heating the sample is employed when higher test temperatures are desired since the large heating currents developed initially can cause local melting in the sample before good thermal conduction has been established.

Also indicated in Fig. 4 is the true sample temperature as indicated by a fine-gage k-type thermocouple (0.127 mm wire diameter) that has been spot-welded onto the sample surface. True temperature is measured most accurately, at present, using the thermocouple method since the NIMPY signal cannot provide a reliable estimate since the sample emissivity is unknown and probably varies during the test due to oxidation [6]. As Fig. 4 shows, the thermocouple response is fast, resulting in no appreciable lag in the true temperature measurement during pulse-heating. An additional benefit of using the thermocouple is that it usually survives the impact event and therefore continues to provide data as the sample cools. Knowledge of the sample cooling history, along with a post-test microstructural analysis of the sample, can be used to deduce the microstructural state of the sample at the time of the impact, which is critical for understanding the non-equilibrium mechanical behavior of metals revealed by this measurement technique. Figure 5 shows the same test as Fig. 4 but in greater detail near the impact time, showing how the heating current can be extinguished within a few milliseconds of the arrival of the compression pulse. It is important to de-energize the heating circuit so that potentially damaging electrical arcing can be prevented from ruining the bars. Precise timing between current shutoff and the impact time is achieved by using the projectile velocity sensors as a trigger signal (see Fig. 1).

Temperature Measurement and Uncertainties

As discussed earlier, measuring the thermodynamic temperature of the sample using pyrometry is problematic because the emissivity of the sample, which depends on oxidation and surface roughness, is unknown and potentially variable. Although the operating wavelength band of the NIMPY makes it less sensitive to uncertainties in emissivity [2], errors in temperature due to unknown emissivity can be substantial and difficult to quantify. Therefore, thermodynamic temperatures are measured using a thermocouple welded directly onto the sample. The uncertainty in the thermocouple reading is estimated at ±4°C (2σ). However, this uncertainty does not reflect the variation in the temperature of the sample through its volume, which is due to minor non-uniformities in the contact conductance. Thermal camera measurements indicate that the sample radiance temperature varies by ±20°C (2σ) when the sample is properly installed (see Fig. 3). The combined uncertainty in true temperature is thus increased to ±20°C (2σ) to reflect temperature variability in the sample.

Occasionally, the temperature history of the sample must be determined from the NIMPY signal because electrical contamination renders the thermocouple signal unreliable before the heating current is extinguished. In this case, the sample emissivity must be determined. Usually the thermocouple reading becomes reliable after the heating circuit is extinguished, so the emissivity can be estimated by

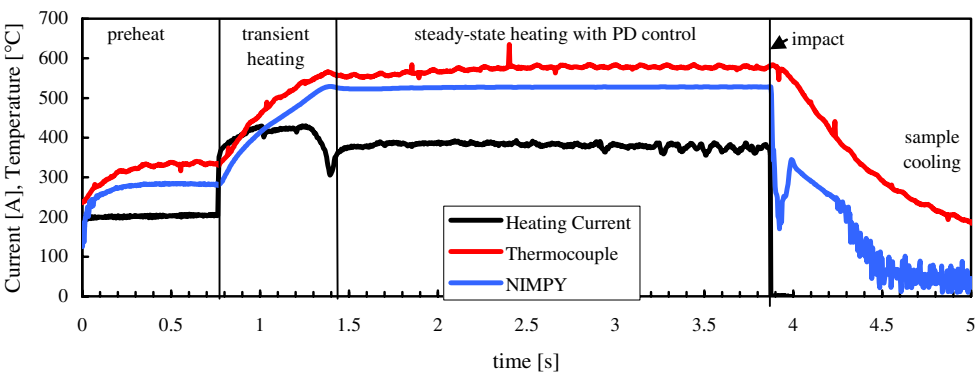

Fig. 4 Power dissipation history and sample temperature history for typical pulse-heating experiment

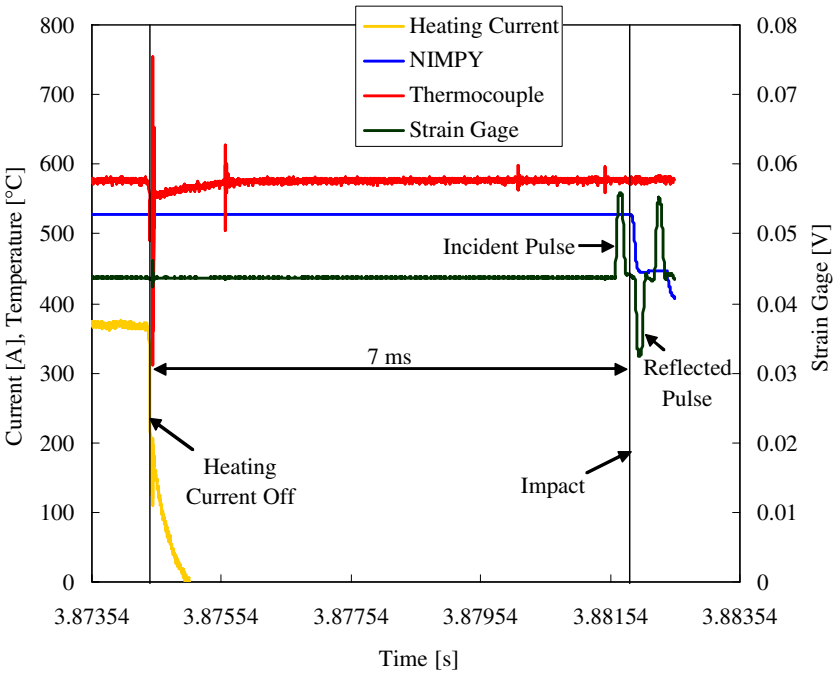

Fig. 5 Sensor data near impact for the experiment shown in Fig. 4 indicating the time delay between current shutoff and the compression pulse arrival at the sample

comparing the thermocouple signal and the radiance temperature measured by the NIMPY. The uncertainty in true temperature is therefore limited by the accuracy of the NIMPY and the uncertainty in the emissivity estimate. For the NIMPY, uncertainties due to resolution, noise and drift in the NIMPY and data acquisition hardware are estimated in Table 1. The NIMPY was calibrated using a blackbody furnace between 300°C and 1,000°C using detector integration times that were the same as those used in the rapid heating experiments. The blackbody furnace accuracy is ±2.5°C. Uncertainties due to the fitting equation are a maximum of ±2°C. The total estimated uncertainty in the radiance temperature measurement, determined by adding in quadrature the individual uncertainties listed in Table 1, is 21°C. Again this uncertainty is dominated by the variability of the sample temperature indicated by the thermal camera. Accounting for the uncertainty in the emissivity, which depends in turn on the thermocouple measurement uncertainty, the overall true temperature uncertainty increases to ±28°C. If the emissivity varies with time, as it may from oxidation growth, the accuracy of the true temperature measurement will deteriorate accordingly the farther away from the impact time one gets. As shown in Fig. 4, however, the thermocouple signal tends to lie roughly parallel to the NIMPY signal over the latter portion of the test, indicating that the emissivity is in fact roughly constant during the controlled-temperature portion of the experiment.

Table 1 Sources of uncertainty in radiance temperature indicated by the NIMPY

Uncertainty source	δT [°C]
Calibration source	2.5
Detector noise	3
Detector resolution	1
Fit equation	2
Repeatability	2
Surface uniformity	20
Combined total uncertainty (2σ)	21

The uncertainty indicated in Table 1 is reliable when the sample is carefully installed. Misaligned foil pads can produce temperature gradients in the sample that are much larger than this uncertainty level, however, as shown already in Fig. 3. Gradients of up to 100°C have been observed due to this problem, which causes non-uniform thermal contact between the sample and the bars. In these cases, the stress–strain measurement is invalid. Poor tests can be detected by anomalously high emissivity readings, or by large temperature gradients observed by the thermal camera, and by checking the power consumption during the test for consistency with earlier tests.

Stress–Strain Measurement and Uncertainties

The usual analysis method for deducing the stress–strain response of samples tested with a Kolsky bar is not sufficient for the pulse-heated technique due to the presence of the graphite foil layers. Although thin and soft compared to the test sample, these layers have a pronounced effect on the strain wave signals, making the traditional analysis un-

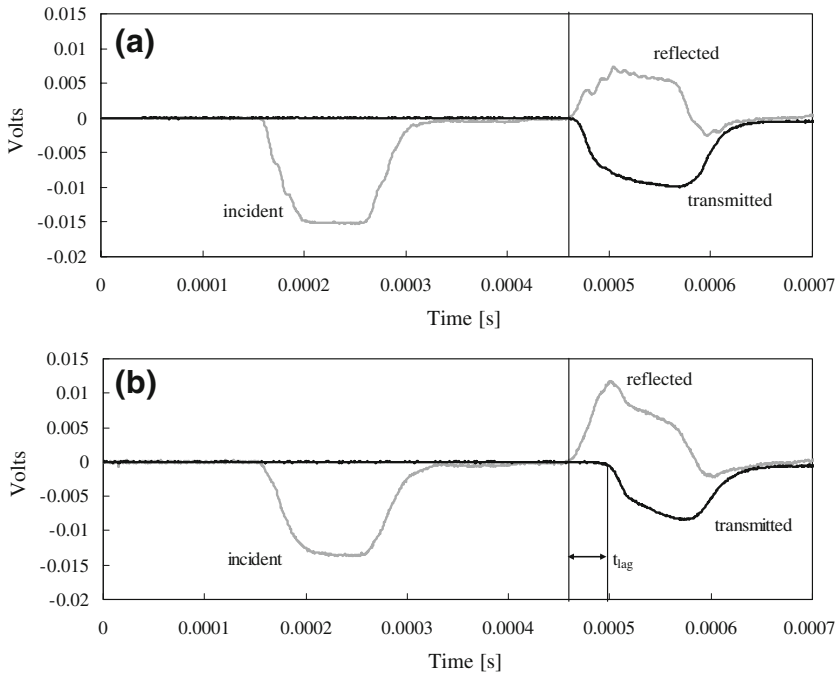

Fig. 6 Strain gage signals obtained from tests (**a**) without foil and (**b**) with foil showing the lag in the transmitted strain signal caused by the foil

suitable. As shown in Fig. 6, the foil causes the transmitted strain signal to lag well behind the reflected wave signal. Without the foil, the transmitted and reflected waves are nearly coincident in time. The lag is caused by the fact that, during the initial contraction of the foil-plus-sample, very little load is transmitted into the second bar because of the softness of the foil. Simply shifting the transmitted strain signal time window to compensate for this lag period does not produce accurate results since it ignores the strength of the foil itself, which becomes significant when the foil becomes highly compressed. A more effective approach is to treat the sample and foil as separately deforming elements. The overall contraction that occurs between the compression bars therefore represents thinning (strain) in the graphite foil plus strain in the sample. The foil response can be predicted independently from the sample response, such that the sample response can then be computed by subtracting the foil contraction from the overall contraction of the foil-plus-sample.

The foil response, as measured in separate Kolsky Bar compression tests, is shown in Fig. 7. Contraction versus true stress was determined by treating the initial deforma-

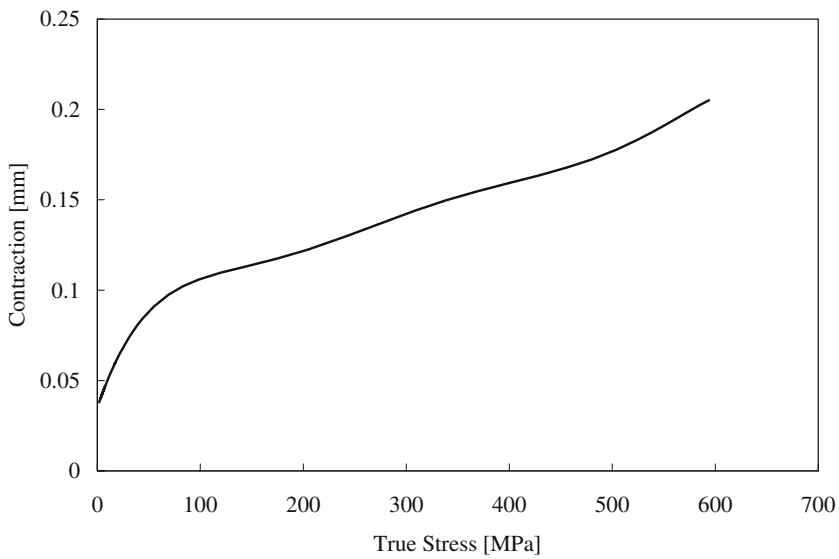

Fig. 7 Averaged displacement versus true stress response of the graphite foil (double thick) determined from Kolsky bar experiments at various striker velocities

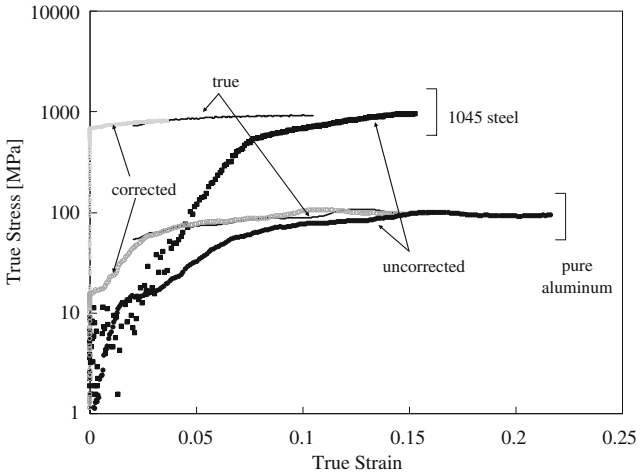

Fig. 8 Stress–strain correction to account for graphite conduction pads. "True" results are obtained from tests conducted without graphite present

tion of the foil as a constant-area contraction to account for collapsing porosity in the foil, which is 50% in its unstressed state. After the porosity has completely collapsed, the foil is assumed to deform with constant volume, such that its cross-sectional area increases in proportion to the strain. The curve in Fig. 7 represents the average of 17 compression tests conducted at three impact velocities (5.4 m/s, 9.8 m/s and 13 m/s) and at temperatures up to 527°C. The uncertainty in this curve is ±12% (2 σ). The response of the foil to elevated temperatures was indistinguishable from its room temperature behavior.

Prior to applying the foil correction algorithm, the strain gage signals must be properly oriented in time with respect to each other. This can be accomplished using the measured compression bar wave speed to determine the appropriate

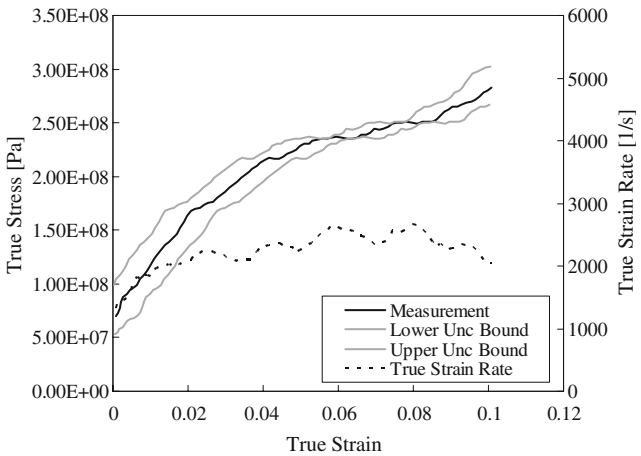

Fig. 9 Uncertainty bounds (±2σ) on true-stress, true-strain measurements obtained using graphite foil (room temperature, pure aluminum sample)

time windows for each gage record as described in [7]. Next, the stress–strain response of the sample is computed by first calculating the contraction of the foil as a function of the stress acting on the sample. The engineering stress on the sample is given by:

$$\sigma_{0,\text{sample}}(t) = \varepsilon_t(t) \cdot \frac{E_{\text{bar}} A_{\text{bar}}}{A_{0,\text{sample}}}. \tag{1}$$

E_{bar} and A_{bar} are the elastic modulus and cross sectional area of the elastic bars, respectively, and $A_{0,\text{sample}}$ is the initial cross sectional area of the sample. The sample contraction, Δl_{sample}, is then computed by subtracting the foil contraction, Δl_{foil}, initially computed using $\sigma_{0,\text{sample}}$, from the overall contraction of the sample plus foil:

$$\Delta l_{\text{sample}}(t) = 2c \int_0^t \varepsilon_r(t)\, d\, t - \Delta l_{\text{foil}}\left(\sigma_{0,\text{sample}}(t)\right). \tag{2}$$

The sample contraction is then used to calculate the true stress and true strain in the sample. Then, the foil contraction is recalculated using the true sample stress. This accounts for deformation in the sample, which affects the stress applied to the foil since the load bearing area of the foil equals that of the sample. After a few iterations, the correct displacements and stresses in the foil and sample can be predicted using this method.

To test the accuracy of this correction method, samples of various yield strengths were tested at room temperature with and without graphite foil present. An accurate correction would yield approximately the same true stress–true strain curves where they overlap in true strain. Figure 8 compares tests performed on 1045 steel and 99.99% pure annealed aluminum, spanning the range of material strengths of interest. Stress–strain curves representing tests conducted with graphite foil but calculated using the traditional wave analysis method that ignores the foil are shown for comparison to illustrate the significant role the foil plays in the measurement. As Fig. 9 shows, the correction method works well across the range of flow stresses of interest. It also reveals that harder materials deform much less when the graphite foil is in place compared the same test without the foil. In the steel test shown in Fig. 8, most of the deformation occurs in the foil. Further, the close correspondence between tests with and without the foil indicates that the foil does not significantly increase the friction during the test. Graphite was chosen for the foil material because, in addition to being conductive, it also serves as a lubricant. Normal tests, which are lubricated with a mineral oil based grease, are very low friction. Had the friction conditions changed appreciably with the foil in place, the stress–strain curve obtained with the foil would not agree well with cures obtained in tests conducted without the foil. Friction tends

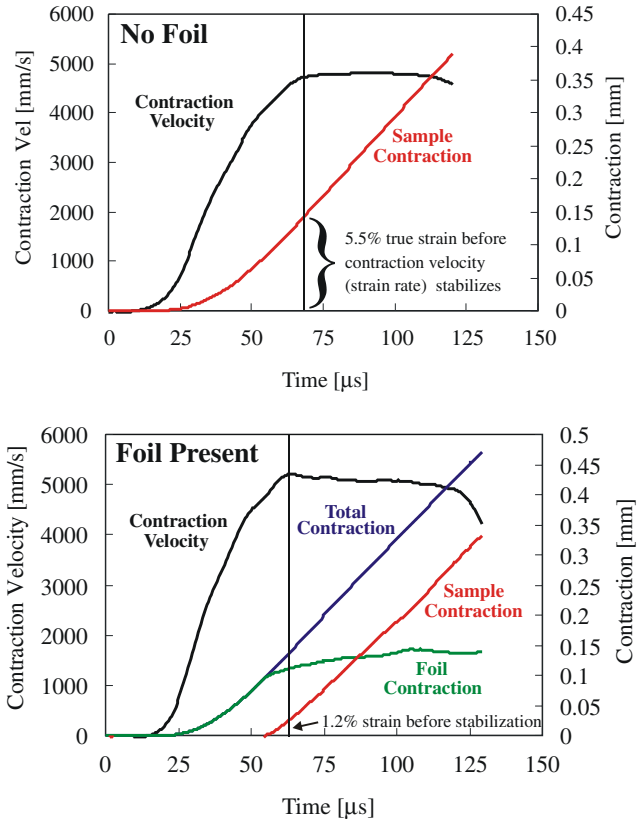

Fig. 10 Comparison of sample contraction prior to strain rate stabilization with and without foil for tests on an aluminum sample

to increase the flow stress indicated by the Kolsky bar test significantly above the real material behavior [8]. Further examination of sample deformation with foil present is planned using high speed digital image correlation [9] to ensure the validity of the pulse-heated Kolsky bar method beyond the evidence presented here.

The uncertainty in the stress–strain data is considerably larger when the graphite foil is employed due to the relatively poor predictability of the foil contraction (±12%). Upper and lower uncertainty bounds are plotted in Fig. 10 for a test on annealed pure aluminum conducted with the foil present. The uncertainty in the yield stress is ±25 MPa, or about 30% of the measured value. Better performance might be obtained by using a foil with a more well-defined mechanical response. However, the excellent thermal properties of this graphite foil make it difficult to replace for pulse-heated testing.

A useful result of conducting tests with graphite foil is that the strain rate applied to the sample stabilizes at far smaller values of plastic strain than for tests done without the foil. In Fig. 9, the strain rate has nearly settled at less than 2% plastic strain. Figure 10 plots the time variation of the overall contraction of the sample plus foil along with the contraction of each material individually and with the total contraction velocity. In this plot, the contraction velocity is analogous to the strain rate. Since the initial deformation is taken mostly by the graphite while the contraction velocity (and strain rate) is rising, the sample begins to deform only after the strain rate has reached a relatively uniform level, particularly compared to tests performed without the foil. A potential therefore exists to accurately measure the yield strength of the test material at high strain rates when the foil is used. This is not possible in traditional Kolsky bar testing, where stress equilibrium and strain rate stabilization are usually not reached until well after the yield point [10].

Of the two, stress equilibrium in the sample is generally established well before the strain rate stabilizes, especially if pulse-shaping is used. Strain rates become stable after the input stress pulse rises to its peak level. In our typical experiment, the pulse rise time is between 20 μs and 40 μs when pulse-shaping is used. Stress equilibrium is believed to be established after the passage of π reverberations of the plastic stress wave in the sample, given by [11]:

$$t \geq \sqrt{\frac{\pi^2 \rho l^2}{\partial \sigma / \partial \varepsilon}} \tag{3}$$

In this equation ρ and l are the density and initial thickness of the sample, respectively, and $\partial\sigma/\partial\varepsilon$ is the slope of the stress–strain curve of the sample material. For steel samples 2 mm thick, stress equilibration is achieved after about 8 μs, assuming a value of 5,400 MPa for the slope of the stress–strain curve at a true strain of 0.005 [12]. So stress equilibrium can be achieved well before the strain rate stabilizes to a constant value. Thus, the strain rate stabilization time is the key factor that limits the ability to measure the small strain response.

Dynamic yield strength measurements can be made without the aid of graphite foil if the strain rate is kept low enough to avoid yielding before the strain rate becomes stable [10]. In the present technique, however, the foil is able to absorb most to all of the deformation while the bar velocity is accelerating during the rising portion of the input stress pulse. As a result, the sample is shielded from deformation as the stress pulse rises, and with proper foil thickness, in principle the yield strength of the sample can be measured regardless of the strain rate magnitude or the sample's strength. With a careful selection of foil thickness, or foil material if pulse heating is not used, it may be possible to obtain valid yield strength data at high strain rates using the Kolsky Bar method for virtually any material.

Conclusions

A new technique is presented for measuring the high strain rate response of metals at high temperatures and subject to high heating rates. The method uses a traditional Kolsky bar modified with a DC electrical pulse heating circuit. Electric current is conducted directly through the specimen using the ends of the compression bars themselves as the electrodes. This method enables the rapid measurement of the high temperature, high strain rate flow stress of metals, and it is uniquely able to probe the non-equilibrium behavior of metals that are subject to rapid thermal excursions. Reliable heating performance is facilitated by the use of thin graphite foil layers placed between the sample and the bars. This foil allows uniform, arc-free heating of the sample by creating a uniform contact conductance across the bar/sample interface. A special strain wave analysis procedure is developed to account for the mechanical influence of the foil in deducing the stress–strain response of the specimen. Uncertainties in the foil deformation response result in somewhat larger uncertainties in the determined stress–strain curves compared to traditional Kolsky bar techniques. Finally, a potentially valuable consequence of using the thin foil to surround the specimen is that it may facilitate more accurate and more versatile dynamic yield strength measurements on metals using Kolsky bar techniques than previously possible.

References

1. Kalpakjian S (1991) Manufacturing processes for engineering materials, 2nd edn. Addison-Wesley, Reading, MA, USA.
2. Gray GT III (1990) Classic split-Hopkinson pressure bar testing. ASM Handbook 8:462–476. Materials Park, Ohio.
3. Basak D, Yoon HW, Rhorer R, Burns TJ, Matsumoto T (2004) Temperature control of pulse heated specimens in a Kolsky Bar apparatus using microsecond time-resolved pyrometry. Int J Thermophys 252:561–574.
4. Frost HJ, Ashby MF (1982) Deformation mechanism maps: the plasticity and creep of metals and ceramics. Pergamon, New York.
5. Lindholm US, Yeakley LM (1968) High strain-rate testing: tension and compression. Exp Mech 8:1–9.
6. DeWitt DP, Nutter GD (1988) Theory and practice of radiation thermometry. Wiley, New York.
7. Lifshitz JM, Leber H (1994) Data processing in the split Hopkinson pressure bar tests. Int J Impact Eng 156:723–733.
8. Bertholf LD, Karnes KH (1975) Two-dimensional analysis of the split Hopkinson pressure bar system. J Mech Phys Solids 23:1–19.
9. Hild F, Roux S (2006) Digital image correlation: from displacement measurement to identification of elastic properties—a review. Strain 42:69–80.
10. Chen W, Song B, Frew DJ, Forrestal MJ (2003) Dynamic small strain measurements of a metal specimen with a split Hopkinson pressure bar. Exp Mech 43:20–23.
11. Davies EDH, Hunter SC (1963) The dynamic compression testing of solids by the method of the split-Hopkinson pressure bar. J Mech Phys Solids 11:155–179.
12. Hertzberg RW (1989) Deformation and fracture mechanics of engineering materials, 3rd edn. Wiley, New York, p 21.